

SFE method using Hermite polynomials: An approach for solving nonlinear mechanical problems with uncertain parameters

J. Baroth^{a,b,*}, L. Bodé^b, Ph. Bressolette^b, M. Fogli^a

^a *LaMI-UBP & IFMA, CUST, Complexe universitaire des Cézeaux, BP 206, 63 174 Aubière Cedex, France*

^b *LGC-UBP, CUST, Complexe universitaire des Cézeaux, BP 206, 63 174 Aubière Cedex, France*

Received 31 May 2005; received in revised form 25 November 2005; accepted 2 February 2006

Abstract

We propose a stochastic finite element method for nonlinear mechanical systems whose uncertain parameters can be modeled as random variables. This method is based on a Gaussian standardization of the problem and on an Hilbertian approximation of the nonlinear mechanical function using Hermite polynomials. The coefficients of the approximation are obtained using a cubic B-spline interpolation of the response function. It provides simple expressions of the response moments. Some of its possibilities are illustrated through four numerical examples concerning one linear problem and three nonlinear problems (elasto-plastic behaviors and contact problem) in which the random parameters are modeled as correlated lognormal random variables. The numerical results obtained attest the relevance of this approach.

© 2006 Elsevier B.V. All rights reserved.

Keywords: Stochastic finite elements; Hilbertian approximation; B-spline interpolation

1. Introduction

Nowadays it is a common practice in structural engineering to use the finite element method to analyze complex mechanical problems. Particularly, nonlinear models are often built even for large industrial problems, whatever the non-linearity type (material, geometrical, etc.). Nevertheless, the number of parameters of these models and therefore the variability and the uncertainty in the determination of their values require the development of new modeling techniques taking into account this random context. The uncertain parameters can be modeled either by random variables (r.v.) or by stochastic fields (elastic modulus of a soil for example). In this work, we only consider vector r.v. without loss of generality because the discretization of random fields always leads to vector r.v.

Using this approach, two kinds of results are expected: either the computation of a reliability index or the achievement of some sensitivity indicators. For both kinds, we often have to estimate statistic moments of the mechanical response. The Monte Carlo simulation methods have first been used [10,23]. Even if these methods have strong advantages (their simplicity, their robustness, their regular improvements [2,4,5]), they usually become time-consuming as the complexity and the size of the embedded deterministic models increase. In order to find an alternative to Monte Carlo simulations, successive probabilistic approaches based on the Finite Element Method (FEM) have been developed for 20 years. These different

* Corresponding author. Address: LaMI-UBP & IFMA, CUST, Complexe universitaire des Cézeaux, BP 206, 63 174 Aubière Cedex, France. Tel.: +33(0)4 73 40 75 46; fax: +33(0)4 73 40 75 26.

E-mail address: baroth@cust.univ-bpclermont.fr (J. Baroth).

approaches have been called Stochastic Finite Element (SFE) Methods [15,19,27]. For example, we can find some perturbation methods [6], the quadrature method [3,27]—based on an extension of the Gauss integrating schemes—or the response surface methods, first used for optimization needs and then in a reliability context [11]. Several methods are based on the discretization of random fields, modeling entry parameters, for example the Spectral Stochastic Finite Element Method [14] or the Weighted Integral Method [8] or others perturbation methods [19,27]. These last SFE Methods are sometimes combined with Monte Carlo simulations [26] and provide an interesting alternative to Monte Carlo simulations for mechanically linear problems. But they cannot be easily extended to the analysis of nonlinear problems. Some studies, for example [1], give interesting results, but only in restricted applications fields. However, the methods where the finite element model is not modified seem to be more promising because the nonlinear deterministic FE calculations are well mastered.

The work presented in this paper is a contribution to the development of SFE Methods to mechanically nonlinear problems. The proposed method can be viewed as a response surface approach. In a reliability context, the approximation of the limit-state function by a polynomial surface is only made around its design point [9,21]. However, when statistical moments have to be computed, it is necessary to approximate the mechanical response in its whole definition domain. This response surface, written in terms of standard Gaussian variables, is an approximation of the mechanical response projection on a finite dimension Hilbert space, which is spanned by an orthogonal Hermite polynomials basis. Such a basis has been widely used for 20 years [12,16]. A difficulty lies in the fact that multiple integrals have to be computed to evaluate the approximation coefficients (see, for example, [13,16,20]). In this paper, we propose a strategy that consists in making a cubic B-spline interpolation of the mechanical response so as to calculate the expansion coefficients. The response surface is then used to compute the approximated statistical moments and to estimate the probability distribution of the response.

The first part of this paper deals with the principle of the method. Then, some possibilities of the approach are investigated through four simple problems: the randomness of the entry parameters is described by one or two correlated log-normal random variables. The first problem is mechanically linear and the three others are nonlinear (elasto-plastic material and contact problem in the fourth application). The quality of approximations is evaluated by comparisons with reference solutions obtained by analytical models, or by Monte Carlo simulations. The influence of the dimension of the projection space and of the interpolation refinement on the calculated moments are eventually studied.

2. Presentation of the method

2.1. Statement of the problem

The study presented in this paper concerns the following problem:

1. We consider a mechanical system whose behavior is nonlinear and described by a finite element model (“black-box” type model).
2. Some scalar parameters y_1, \dots, y_k of the model, gathered in a vector $y = (y_1, \dots, y_k) \in \mathbb{R}^k$, $k \in \mathbb{N}^*$, are uncertain.
3. We are interested in a scalar observation z (displacement, strain, stress, etc.) of the response system, linked to y via a relationship of the form:

$$z = f(y), \quad (1)$$

where f is a measurable function from \mathbb{R}^k into \mathbb{R} completely determined by the finite element model.

4. We want to quantify the effect of the random variability of y on z .
5. With this object in view, we assume that y can be suitably modeled as a \mathbb{R}^k -valued random variable (r.v.) $Y = (Y_1, \dots, Y_k)$ with given absolutely continuous probability distribution P_Y such that $Supp(P_Y) \subseteq def(f)$, where $Supp(P_Y)$ and $def(f)$ denote respectively the support of P_Y and the definition domain of f .
6. In these conditions, f being measurable and \mathbb{R} -valued, z is a scalar r.v. denoted by Z , such that

$$Z = f(Y). \quad (2)$$

7. In accordance with point 4, then we seek to characterize the r.v. Z , given the couple (f, Y) , where Y is defined by its probability distribution P_Y and f by the considered finite element model.

The proposed approach is based on the construction of an Hilbertian approximation of f that allows us to estimate the statistical moments of the r.v. Z ; in particular, its two first moments (mean and variance) will allow us to quantify the effect of the random variability of Y on the second order random variability (i.e. the scattering) of Z . It goes without saying that the full characterization of Z is its probability distribution. On the one hand, considering the specificity of the problem (f is nonlinear and not defined by an explicit analytical expression, k is not necessarily small, and Y is a priori not Gaussian), estimation of this function by using Monte Carlo simulation of the FE model would be very time consuming. On the other

hand, simulation of the Hilbertian approximation will be very cheap, so this approach may be considered in order to build an approximation of the probability distribution.

The first step of this approach consists in rewriting the problem in terms of standardized Gaussian r.v.'s.

2.2. Gaussian standardization

Under little constraining assumptions, that we take as satisfied here, it can be shown that there exists a measurable function T from \mathbb{R}^k into \mathbb{R}^k and a \mathbb{R}^k -valued standard Gaussian r.v. X such that

$$Y = T(X), \tag{3}$$

where the equality in Eq. (3) must be interpreted as an equality of probability distributions. Inserting Eq. (3) in Eq. (2) yields

$$Z = g(X), \tag{4}$$

where g is a measurable function from \mathbb{R}^k into \mathbb{R} such that

$$g = f \circ T. \tag{5}$$

Eq. (4), that expresses Z as a function of standardized Gaussian r.v.'s, defines the working formulation on which the proposed method is based.

Appendix A gives the expression of T when X is lognormal, which is the case in the present work (see applications in Section 3). The general expression of T is given in reference [22].

2.3. Fundamental assumption on g

Let ν_k be the standard Gaussian probability distribution on \mathbb{R}^k and let φ_k be its density with respect to the Lebesgue measure $dx = dx_1 \cdots dx_k$ on \mathbb{R}^k . We have, $\forall x = (x_1, \dots, x_k) \in \mathbb{R}^k$,

$$\nu_k(dx) = \varphi_k(x)dx; \quad \varphi_k(x) = (2\pi)^{-\frac{k}{2}} \exp\left(-\frac{\|x\|^2}{2}\right), \tag{6}$$

where $\|\cdot\|$ denotes the canonical Euclidean norm on \mathbb{R}^k . In the following, we will assume that g is square integrable with respect to ν_k , that is to say that the condition:

$$\int_{\mathbb{R}^k} g^2(x)\nu_k(dx) = \int_{\mathbb{R}^k} g^2(x)\varphi_k(x)dx < +\infty \tag{7}$$

is satisfied. The above integrability requirement is usually satisfied in physical systems.

2.4. Hilbertian approximation of g

Let $L^2(\mathbb{R}^k, \nu_k)$ be the Hilbert space of the ν_k -square integrable functions from \mathbb{R}^k into \mathbb{R} , equipped with the inner product $((\cdot, \cdot))$ and the associated norm $\|\cdot\|$, such that, $\forall f_1, f_2 \in L^2(\mathbb{R}^k, \nu_k)$,

$$((f_1, f_2)) = \int_{\mathbb{R}^k} f_1(x)f_2(x)\nu_k(dx) = \int_{\mathbb{R}^k} f_1(x)f_2(x)\varphi_k(x)dx, \tag{8}$$

$$\|f_1\| = ((f_1, f_1))^{\frac{1}{2}}. \tag{9}$$

Let $(H_\alpha(x), \alpha \in \mathbb{N}^k)$ be the family of Hermite polynomials on \mathbb{R}^k and let $(h_\alpha(x), \alpha \in \mathbb{N}^k)$ be the associated standardized family, such that, $\forall x \in \mathbb{R}^k$ and $\forall \alpha \in \mathbb{N}^k$, $h_\alpha(x) = (\alpha!)^{-\frac{1}{2}}H_\alpha(x)$ (see Appendix B), where $\alpha = (\alpha_1, \dots, \alpha_k) \in \mathbb{N}^k$, $k \in \mathbb{N}^*$, is a k -order multi-index with length $|\alpha| = \alpha_1 + \dots + \alpha_k$.

Given that $(h_\alpha(x), \alpha \in \mathbb{N}^k)$ forms an orthonormal basis of $L^2(\mathbb{R}^k, \nu_k)$ and considering that, from Eq. (7), the function g belongs to this space, we can write, $\forall x \in \mathbb{R}^k$,

$$g(x) = \sum_{|\alpha|=0}^{+\infty} G_\alpha h_\alpha(x) = \sum_{|\alpha|=0}^{+\infty} g_\alpha H_\alpha(x), \tag{10}$$

where

$$G_\alpha = ((g, h_\alpha)) = \int_{\mathbb{R}^k} g(x)h_\alpha(x)\varphi_k(x)dx \tag{11}$$

and

$$g_\alpha = \frac{1}{\alpha!} ((g, H_\alpha)) = \frac{1}{\alpha!} \int_{\mathbb{R}^k} g(x) H_\alpha(x) \varphi_k(x) dx. \quad (12)$$

A M -order Hilbertian approximation g^M of g is then obtained by truncating the expansion (10) at a fixed order $M \in \mathbb{N}^*$:

$$g^M(x) = \sum_{|\alpha|=0}^M g_\alpha H_\alpha(x). \quad (13)$$

Recall that $H_\alpha(x)$ is given by (see Appendix B):

$$H_\alpha(x) = \prod_{i=1}^k H_{\alpha_i}(x_i), \quad (14)$$

where $x = (x_1, \dots, x_k) \in \mathbb{R}^k$ and, $\forall i \in \{1, \dots, k\}$, $H_{\alpha_i}(x_i)$ is the α_i -order Hermite polynomial on \mathbb{R} .

Thus, determining a M -order Hilbertian approximation of g reduces to estimate the coefficients $(g_\alpha, |\alpha| = 0, \dots, M)$ given by Eq. (12), which can be rewritten:

$$g_\alpha = \frac{1}{\alpha!} \langle g(X) H_\alpha(X) \rangle, \quad (15)$$

where $\langle \cdot \rangle$ denotes the mathematical expectation. In the following, M will be called ‘‘approximation order’’.

2.5. Calculating the approximation coefficients

Calculating the coefficients g_α given by Eqs. (12)–(15) represents the most important and most delicate step of the method. We could have used Monte Carlo, quasi Monte Carlo or Modified Monte Carlo methods [2,4,5,10,23] to carry out this calculation. This strategy would have required much calls to function g and has been excluded for practical reasons. Other methods [13,16] could also be used, but again, they do not seem to realize the best compromise between the quality of the approximation and its cost. This is the reason why we have chosen another approach. It consists in replacing g in Eqs. (12)–(15) with a piecewise polynomial approximation constructed from a cubic B-spline interpolation [7].

Let us suppose that this approximation, denoted by S , has been constructed. Then, according to Eqs. (12)–(15), the coefficients g_α are approximated by

$$g_\alpha \simeq \tilde{g}_\alpha = \frac{1}{\alpha!} \langle S(X) H_\alpha(X) \rangle = \frac{1}{\alpha!} \int_{\mathbb{R}^k} S(x) H_\alpha(x) \varphi_k(x) dx, \quad (16)$$

and $g^M(x)$ in (13) is approximated by

$$g^M(x) \simeq \tilde{g}^M(x) = \sum_{|\alpha|=0}^M \tilde{g}_\alpha H_\alpha(x). \quad (17)$$

The obvious interest of this approach is that, once the approximation S has been obtained, calling g is not required to calculate the coefficients \tilde{g}_α . Consequently, any numerical method (Monte Carlo, quadrature, etc.) can be used. For example, for small values of the problem dimension, a Gauss–Legendre integration scheme could be used.

The determination of S constitutes the main cost of this strategy. The graph of such an approximation is composed of n^k hyper-arcs, that is of n^k hyper-surfaces restricted to bounded hypercubes of \mathbb{R}^k , where n is the number of interpolation arcs in each space direction and k the number of input r.v. For the sake of simplicity, only uniformly distributed interpolation points are considered in this first work. Determining S requires to define $N_I = (n + 1)^k$ interpolation points and therefore to call N_I times the function g (see Appendix C). Even if we optimize the location of these interpolation points, the number of deterministic computations increase exponentially with the number of input r.v., as long as a tensor-product quadrature formula is used. This is the main reason why the proposed approach is limited to problems involving a small number of uncertain parameters, which represent however a large field of engineering problems. The use of integration schemes more suitable for high dimensional integrals calculations, as Smolyak quadrature [25], would probably allow to consider problems involving a larger number of r.v. However, it seems unrealistic to apply such a method (like other surface response methods) to situations where stochastic fields are to be considered.

2.6. Approximation of moments of Z

The coefficients \tilde{g}_α being calculated, let us introduce the scalar r.v. \tilde{Z}_M such that

$$\tilde{Z}_M = \tilde{g}^M(X) = \sum_{|\alpha|=0}^M \tilde{g}_\alpha H_\alpha(X) \quad (18)$$

whose N -order moment, for any N in \mathbb{N}^* , is given by

$$\tilde{\mu}_{M,N} = \langle \tilde{Z}_M^N \rangle = \sum_{|\alpha^1|=0}^M \cdots \sum_{|\alpha^N|=0}^M \tilde{g}_{\alpha^1} \cdots \tilde{g}_{\alpha^N} \left\langle \prod_{j=1}^N H_{\alpha^j}(X) \right\rangle, \tag{19}$$

where, $\forall j \in \{1, \dots, N\}$, $\alpha^j = (\alpha_1^j, \dots, \alpha_k^j) \in \mathbb{N}^k$ is a k -order multi-index. For any N in \mathbb{N}^* , the corresponding moment $\mu_N = \langle Z^N \rangle$ of the r.v. Z defined by Eq. (4) can then be approximated by $\tilde{\mu}_{M,N}$:

$$\mu_N \simeq \tilde{\mu}_{M,N}. \tag{20}$$

Using the orthogonality properties of Hermite polynomials, the formula (19) can be easily computed. As an example, for $N = 1$ and $N = 2$, we obtain

$$\mu_1 = \langle Z \rangle \simeq \tilde{\mu}_{M,1} = \sum_{|\alpha|=0}^M \tilde{g}_\alpha \delta_{\alpha,0} = \tilde{g}_0, \tag{21}$$

$$\mu_2 = \langle Z^2 \rangle \simeq \tilde{\mu}_{M,2} = \sum_{|\alpha^1|=0}^M \sum_{|\alpha^2|=0}^M \tilde{g}_{\alpha^1} \tilde{g}_{\alpha^2} \alpha^1! \delta_{\alpha^1, \alpha^2}. \tag{22}$$

Let us suppose now that more than one scalar observation of the response is considered (see for example application in Section 3.4) and let be l the number of these observations: Z is then a vector r.v. $Z = (Z_1, \dots, Z_l)$. The covariance of a couple (Z_I, Z_J) is given by

$$\text{Cov}(Z_I, Z_J) \simeq \sum_{|\alpha^1|=0}^M \sum_{|\alpha^2|=0}^M \tilde{g}_{\alpha^1}^I \tilde{g}_{\alpha^2}^J \alpha^1! \delta_{\alpha^1, \alpha^2}, \tag{23}$$

where $Z_I \simeq \tilde{Z}_{M,I} = \sum_{|\alpha|=0}^M \tilde{g}_\alpha^I H_\alpha(X)$, $Z_J \simeq \tilde{Z}_{M,J} = \sum_{|\alpha|=0}^M \tilde{g}_\alpha^J H_\alpha(X)$.

Let be P the effective number of terms in the expansion (13) or (17); P is always greater than M (for $k = 1$, $P = M + 1$, for $k = 2$, $P = \frac{(M+1)(M+2)}{2}$, ...) and is called ‘‘truncation order’’. For computational purposes, each Hermite polynomial on \mathbb{R}^k involved in (13) or (17) can be associated to an integer index j such that $0 \leq j \leq P - 1$. So (18) can also be written:

$$\tilde{Z}_M = \sum_{j=0}^{P-1} \tilde{g}_j H_j(X) \tag{24}$$

and, remembering that $\langle Z \rangle \simeq \tilde{g}_0$ (see Eq. (21)), an approximation of any centered N -order moment of Z can be

$$\langle Z - \langle Z \rangle \rangle^N = \bar{\mu}_N \simeq \langle \tilde{Z}_M - \tilde{g}_0 \rangle^N = \tilde{\mu}_{M,N} = \left(\sum_{j=1}^{P-1} \tilde{g}_j H_j(X) \right)^N. \tag{25}$$

After some algebra, it can be written that

$$\tilde{\mu}_{M,N} = \underbrace{\sum_{i_1=0}^N \sum_{i_2=0}^{i_1} \cdots \sum_{i_{P-2}=0}^{i_{P-3}}}_{P-2 \text{ sums}} A_{i_1 i_2 \dots i_{P-2}, N} \left\langle H_1^{(N-i_1)} H_2^{(i_1-i_2)} \cdots H_{P-2}^{(i_{P-3}-i_{P-2})} H_{P-1}^{(i_{P-2})} \right\rangle, \tag{26}$$

where

$$A_{i_1 i_2 \dots i_{P-2}, N} = \binom{N}{i_1} \binom{i_1}{i_2} \cdots \binom{i_{P-3}}{i_{P-2}} \times \tilde{g}_1^{(N-i_1)} \tilde{g}_2^{(i_1-i_2)} \cdots \tilde{g}_{P-2}^{(i_{P-3}-i_{P-2})} \tilde{g}_{P-1}^{(i_{P-2})}$$

and with $\binom{i}{j} = \frac{i!}{j!(i-j)!}$ the binomial coefficient.

So the computation of (26) leads to the evaluation of the following kind of expectations:

$$\left\langle \prod_{j=1}^{P-1} (H_j(X))^{\beta_j} \right\rangle = \prod_{i=1}^k \left\langle \prod_{j=1}^{P-1} (H_{\alpha_j,i}(X_i))^{\beta_j} \right\rangle, \tag{27}$$

where $H_j(X) = \prod_{i=1}^k H_{\alpha_j,i}(X_i)$, with H_j Hermite polynomial on \mathbb{R}^k and $H_{\alpha_j,i}$ associated Hermite polynomials on \mathbb{R} .

A set of Fortran subroutines has been developed in order to compute *exactly* these statistical moments,¹ whatever the order N and the dimension k . Thus, we can reach our goal, which was to obtain numerical approximations of the statistical

¹ In practice, it is especially interesting to evaluate the well-known *skewness* (β_1) and *kurtosis* (β_2), respectively defined as: $\beta_1 = \frac{\bar{\mu}_3}{\sigma^3}$, $\beta_2 = \frac{\bar{\mu}_4}{\sigma^4}$, where σ , $\bar{\mu}_3$ and $\bar{\mu}_4$ are the standard deviation and the 3-order and 4-order centered moments.

moments at a low cost. The knowledge of these approximated statistical moments could be used to approximate the probability density function of the r.v. Z . In practice, we preferred to estimate this function by performing Monte Carlo simulations of the M -order approximation \tilde{g}^M of g (17) (see applications).

To finish, consider the scalar r.v.:

$$Z_M = g^M(X) = \sum_{|\alpha|=0}^M g_\alpha H_\alpha(X) \quad (28)$$

which differs from \tilde{Z}_M in that, according to Eq. (16), the coefficients of the \tilde{Z}_M -expansion (18) are approximations of those of the expansion (28). Then, it can be shown that the r.v. Z_M , with g_α given by Eqs. (12)–(15) for α such as $0 \leq |\alpha| \leq M$, is the best approximation in the mean-square sense of Eq. (4). As a result, if the coefficients \tilde{g}_α are good approximations of the coefficients g_α , we are sure that the approximations of the moments μ_N of Z by the moments $\tilde{\mu}_{M,N}$ of \tilde{Z}_M are correct, at least up to the second order (i.e. for $N \leq 2$).

3. Applications

In order to illustrate some possibilities of the proposed method, we propose four applications focused on the calculation of the statistical moments of the system response and on the estimation of the Probability Density Function (PDF) of the marginal laws of the response r.v. The influence of the variability of the uncertain parameters on the response system is also studied. The uncertain parameters are modeled as lognormal r.v.'s; these r.v. are correlated if more than one is considered. The first presented example deals with a mechanically linear problem. Thanks to its simplicity, the exact analytical expressions of the target moments can be established. The other examples concern some nonlinear problems for which the calculation of the target moments requires using a Monte Carlo procedure.

3.1. Application 1: Bar under axial load

We consider a homogeneous rectilinear bar with constant section, embedded at one end and submitted to an axial load at the other one (see Fig. 1).

We are interested in the longitudinal elastic displacement z of the final section, given by

$$z = \frac{FL}{ES}, \quad (29)$$

where F is the tensile axial load, S is the area of the cross-section, L is the length of the bar and E is the Young modulus of the constitutive material.

The uncertain parameters of the model are L and S , respectively denoted by y_1 and y_2 . Hence

$$z = ay_1y_2^{-1}; \quad a = E^{-1}F. \quad (30)$$

The parameters E and F are deterministic and equal to

$$E = 2.1 \times 10^{11} \text{ Pa}; \quad F = 10^6 \text{ N}.$$

The couple $y = (y_1, y_2)$ is modeled as a two-dimensional lognormal r.v. $Y = (Y_1, Y_2)$ with characteristics:

Mean of Y_1 : $m_{Y_1} = \langle Y_1 \rangle = 1 \text{ m}$; Variance of Y_1 : $\sigma_{Y_1}^2 = \langle (Y_1 - m_{Y_1})^2 \rangle = m_{Y_1}^2 v_{Y_1}^2$.

Mean of Y_2 : $m_{Y_2} = \langle Y_2 \rangle = 2 \times 10^{-4} \text{ m}^2$; Variance of Y_2 : $\sigma_{Y_2}^2 = \langle (Y_2 - m_{Y_2})^2 \rangle = m_{Y_2}^2 v_{Y_2}^2$.

Covariance of Y_1 and Y_2 : $C_{Y_1Y_2} = \langle (Y_1 - m_{Y_1})(Y_2 - m_{Y_2}) \rangle = m_{Y_1}m_{Y_2}v_{Y_1}v_{Y_2}\rho_{Y_1Y_2}$, where v_{Y_1} (resp. v_{Y_2}) is the coefficient of variation of Y_1 (resp. Y_2) and $\rho_{Y_1Y_2}$ is the coefficient of correlation of the couple (Y_1, Y_2) .

As a result, z is a scalar r.v. that we shall denote by Z from now on and which is such that

$$Z = aY_1Y_2^{-1}. \quad (31)$$

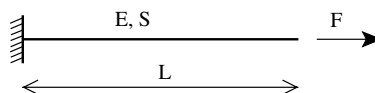


Fig. 1. Bar under axial load.

It can be easily shown that this r.v. is lognormal, with mean m_Z and coefficient of variation v_Z given by

$$m_Z = am_{Y_1}m_{Y_2}^{-1}(1 + v_{Y_2}^2)(1 + v_{Y_1}v_{Y_2}\rho_{Y_1Y_2})^{-1}, \tag{32}$$

$$v_Z^2 = (1 + v_{Y_1}^2)(1 + v_{Y_2}^2)(1 + v_{Y_1}v_{Y_2}\rho_{Y_1Y_2})^{-2} - 1. \tag{33}$$

The scattering of the response results from the variability of the random parameters Y_1 (the length) and Y_2 (the section area). It is characterized by the coefficient of variation v_Z , and therefore, according to Eq. (33), only depends on v_{Y_1} , v_{Y_2} and $\rho_{Y_1Y_2}$.

Approximations of the two first moments of Z are driven by two parameters: the approximation order M and the number N_I of B-spline interpolation points. For given values of M and N_I , the approximations of the mean and of the standard deviation of Z are respectively denoted by $\tilde{m}_Z(M, N_I)$ and $\tilde{\sigma}_Z(M, N_I)$. These statistics are compared to the corresponding exact statistics m_Z and σ_Z given by Eqs. (32) and (33) (where $\sigma_Z = m_Z v_Z$) by means of the relative error rates:

$$\varepsilon_m(M, N_I) = \frac{100[m_Z - \tilde{m}_Z(M, N_I)]}{m_Z}; \quad \varepsilon_\sigma(M, N_I) = \frac{100[\sigma_Z - \tilde{\sigma}_Z(M, N_I)]}{\sigma_Z}.$$

In fact, according to Eq. (21), $\tilde{m}_Z(M, N_I)$ does not depend on M , and consequently neither does $\varepsilon_m(M, N_I)$. It will be denoted by $\varepsilon_m(N_I)$ in the following. Fig. 2 shows the variation of $\varepsilon_m(N_I)$ with N_I , for $v_{Y_1} = v_{Y_2} = 0.1$ and $\rho_{Y_1Y_2} = 0.8$.

For the same values of v_{Y_1} , v_{Y_2} and $\rho_{Y_1Y_2}$, Fig. 3 depicts the variation of $\varepsilon_\sigma(M, N_I)$ with M , for several values of N_I . On these figures, we can see that the approximation of the mean is good, even for small values of N_I . However, the approximated standard deviation does not converge on the exact one if N_I is too small, that is if the interpolation refinement is not sufficient. Nevertheless, for values of N_I allowing convergence, it can be noticed that this one is fast and leads to very good approximations.

For any fixed value of the couple (M, N_I) , the approximation of the coefficient of variation v_Z of Z is denoted by $\tilde{v}_Z(M, N_I)$. For $M = 2$ and for two values of N_I (25 and 36), Figs. 4 and 5 show the variation of $\tilde{v}_Z(M, N_I)$ with, respectively (a) v_{Y_1} , for $v_{Y_2} = 0.1$ and $\rho_{Y_1Y_2} = 0.8$ (Fig. 4), (b) $\rho_{Y_1Y_2}$, for $v_{Y_1} = v_{Y_2} = 0.1$ (Fig. 5). The values $N_I = 25$ and $N_I = 36$ correspond respectively to 4 and 5 B-spline interpolation arcs in each space direction. The corresponding evolutions of the exact coefficient of variation v_Z , given by Eq. (33), are plotted on the same figures. The comparison of these graphs shows a good agreement between exact and approximated results. We can also observe that this agreement improves when N_I increases, that is when the accuracy of the interpolation improves.

3.2. Application 2: Elasto-plastic truss

Now we consider a three-bar truss (see Fig. 6) submitted to a deterministic load F applied on its bottom node. Lateral bars have the same Young modulus E_1 and the same length $L/\cos\alpha$, where L is the length of the central bar, which is composed of a material with Young modulus E_2 . The three bars have the same section, with area S .

We are interested in the vertical displacement z of the bottom node, calculated under the assumption that the mechanical behavior of the constituent materials is elasto-plastic.

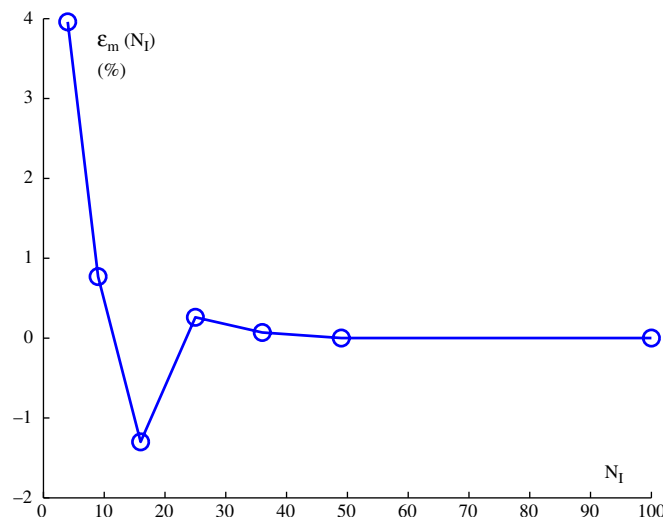


Fig. 2. Variation of the error rate $\varepsilon_m(N_I)$ with the number N_I of interpolation points ($v_{Y_1} = v_{Y_2} = 0.1$, $\rho_{Y_1Y_2} = 0.8$).

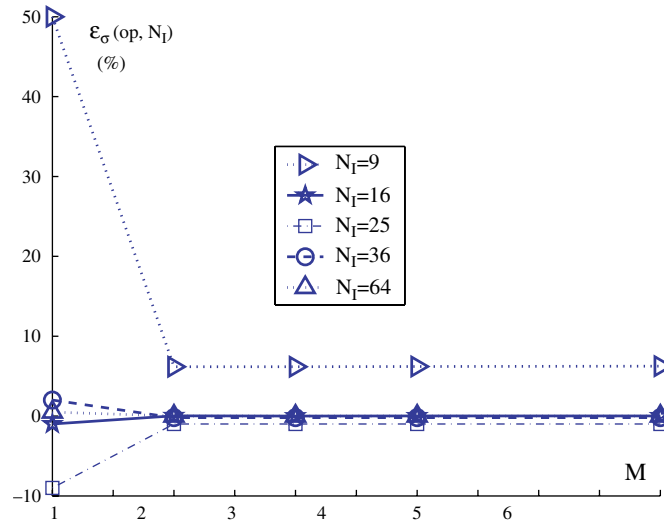


Fig. 3. Variation of the error rate $\epsilon_\sigma(M, N_I)$ with the approximation order M for some values of the number N_I of interpolation points ($v_{Y_1} = v_{Y_2} = 0.1$, $\rho_{Y_1Y_2} = 0.8$).

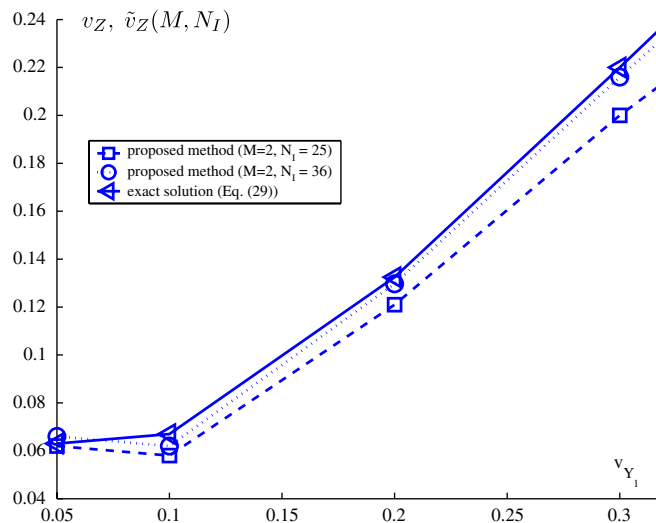


Fig. 4. Variation of the coefficient of variation of Z with v_{Y_1} ($v_{Y_2} = 0.1$, $\rho_{Y_1Y_2} = 0.8$, $M = 2$).

The uncertain parameters of the mechanical model are the Young modulus E_1 and E_2 , denoted by y_1 and y_2 respectively. The couple $y = (y_1, y_2)$ is modeled as a two-dimensional lognormal r.v. $Y = (Y_1, Y_2)$ with characteristics:

- Mean of Y_1 : $m_{Y_1} = 2 \times 10^{10}$ Pa; Standard deviation of Y_1 : $\sigma_{Y_1} = m_{Y_1} v_{Y_1}$.
- Mean of Y_2 : $m_{Y_2} = 2 \times 10^{10}$ Pa; Standard deviation of Y_2 : $\sigma_{Y_2} = m_{Y_2} v_{Y_2}$.
- Covariance of Y_1 and Y_2 : $C_{Y_1Y_2} = m_{Y_1} m_{Y_2} v_{Y_1} v_{Y_2} \rho_{Y_1Y_2}$ where v_{Y_1} (resp. v_{Y_2}) is the coefficient of variation of Y_1 (resp. Y_2) and $\rho_{Y_1Y_2}$ is the coefficient of correlation of the couple (Y_1, Y_2) .

The other parameters of the model, namely L, S, α, F, f_y (yield stress) and E_p (plastic modulus) are deterministic and equal to

$$L = 1 \text{ m}; \quad S = 20 \times 10^{-4} \text{ m}^2; \quad \alpha = \pi/4,$$

$$F = 25 \times 10^4 \text{ N}; \quad f_y = 6 \times 10^7 \text{ Pa}; \quad E_p = 0.7 m_{Y_1}.$$

Under these conditions, the displacement z is a scalar r.v. that we shall denote by Z from now on and which is such that: $Z = f(Y)$, where f is a nonlinear mapping from (\mathbb{R}_+^2) into \mathbb{R} whose expression can be analytically established in this particular case (see [17]).

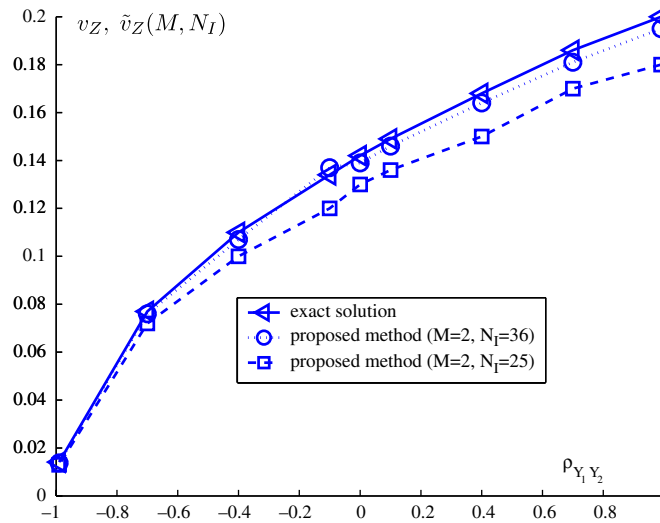


Fig. 5. Variation of the coefficient of variation of Z with $\rho_{Y_1 Y_2}$ ($v_{Y_1} = v_{Y_2} = 0.1$, $M = 2$).

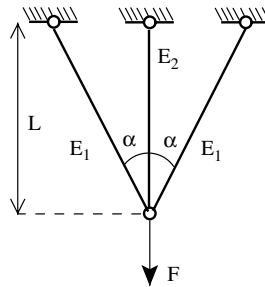


Fig. 6. Elasto-plastic truss.

We are interested in the mean m_Z and the standard deviation σ_Z of this r.v. As explained in the first application, the approximation of m_Z , denoted by $\tilde{m}_Z(N_I)$, only depends on N_I and the approximation of σ_Z , denoted by $\tilde{\sigma}_Z(M, N_I)$, depends on M and N_I . Table 1 shows the variation of $\tilde{m}_Z(N_I)$ with N_I , for $v_{Y_1} = v_{Y_2} = 0.3$ and $\rho_{Y_1 Y_2} = 1$ (we consider such largest values of v_{Y_1} and v_{Y_2} in order to verify the numerical convergence of the method, even for large coefficients of variation).

The variation of $\tilde{\sigma}_Z(M, N_I)$ with M is plotted in Fig. 7 for the same values of v_{Y_1} , v_{Y_2} and $\rho_{Y_1 Y_2}$, and for three values of N_I : 9, 16 and 81, corresponding respectively to 2, 3 and 8 interpolation B-spline arcs in each space direction.

In each case, $\tilde{m}_Z(N_I)$ and $\tilde{\sigma}_Z(M, N_I)$ are compared with their respective targets \hat{m}_Z and $\hat{\sigma}_Z$ estimated from 10^5 Monte Carlo simulations. We can observe that these results are consistent with those of the first application, that is: (a) the mean approximation rapidly converges to the target value, (b) for small values of N_I , the standard deviation approximation does not converge to the target value, and (c) for values of N_I for which the convergence is possible, this one is very fast and leads to very good approximations.

We denote by $\tilde{v}_Z(M, N_I)$ the coefficient of variation of Z provided by the proposed method and by \hat{v}_Z the corresponding target statistic obtained from Monte Carlo simulations: $\tilde{v}_Z(M, N_I) = \tilde{\sigma}_Z(M, N_I) / \tilde{m}_Z(N_I)$, $\hat{v}_Z = \hat{\sigma}_Z / \hat{m}_Z$. For $M = 6$, $v_{Y_2} = 0.1$, $\rho_{Y_1 Y_2} = 0.8$ and for two values of N_I : 25 and 36, corresponding respectively to 4 and 5 B-spline interpolation arcs in each space direction, Fig. 8 depicts the variation of $\tilde{v}_Z(M, N_I)$ with v_{Y_1} and compares this evolution with the one of the target \hat{v}_Z .

Table 1
Variation of the mean of Z with the number N_I of B-spline interpolation points ($v_{Y_1} = v_{Y_2} = 0.3$, $\rho_{Y_1 Y_2} = 1$)

	N_I				
	9	16	25	49	81
Proposed method: $\tilde{m}_Z(N_I) (\times 10^{-3} \text{ m})$	4.32	3.75	4.02	4.10	4.09
Monte Carlo simulations: $\hat{m}_Z (\times 10^{-3} \text{ m})$			4.09		

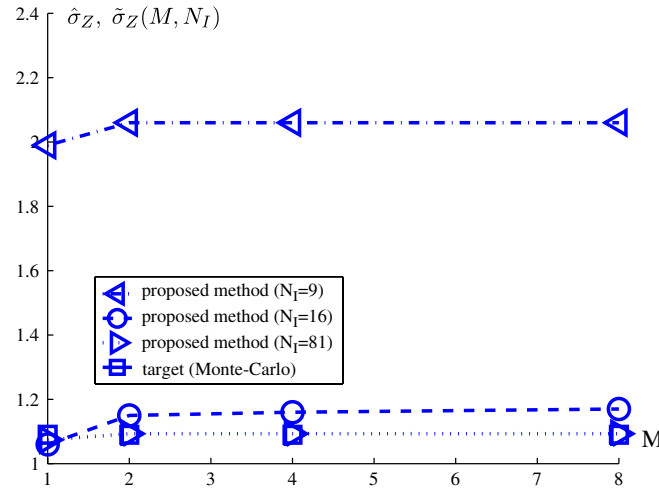


Fig. 7. Variation of the standard deviation of Z with the approximation order M ($v_{Y_1} = v_{Y_2} = 0.3, \rho_{Y_1 Y_2} = 1$).

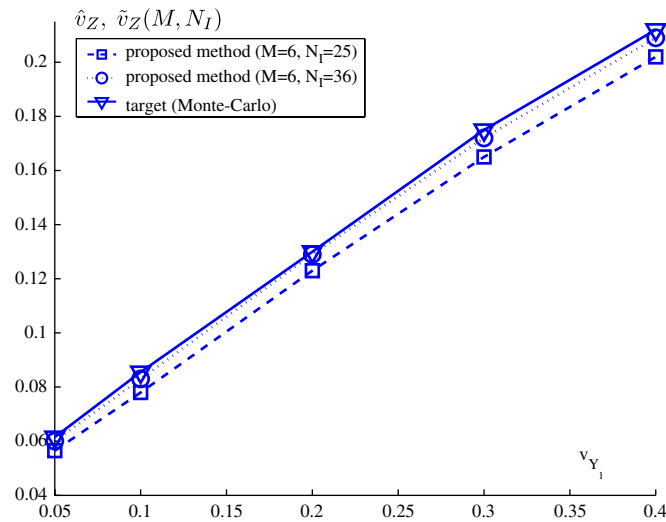


Fig. 8. Variation of the coefficient of variation of Z with v_{Y_1} ($v_{Y_2} = 0.1, \rho_{Y_1 Y_2} = 0.8, M = 6$).

Again, these results corroborate those of the previous application: a good agreement is observed between approximations and targets and this agreement highly improves when N_I increases.

3.3. Sphere under internal pressure

This application deals with a hollow sphere under internal pressure (see Fig. 9). The geometrical and mechanical parameters of the model are the internal and external radius a and b , the Young modulus E , the Poisson ratio ν , the yield stress f_y and the internal pressure p . The constituent material is supposed to be elastic perfectly plastic.

The random parameter of the problem is the Young modulus E , afterwards denoted by y and modeled as a lognormal r.v. Y with characteristics: $m_Y = 2 \times 10^{11}$ Pa, $\sigma_Y = m_Y v_Y$.

The other parameters are assumed to be deterministic and equal to: $\nu = 0.3, a = 1$ mm, $b = 2$ mm, $f_y = 3 \times 10^8$ Pa, $p = 3.589 \times 10^8$ Pa. We are interested here in the radial plastic displacement z at any point of the internal outline. The deterministic solution of this problem is known [18]. In the random case, the solution is a scalar r.v. Z given by

$$Z = f(Y), \tag{34}$$

where f is a mapping from \mathbb{R}_+^* into \mathbb{R} , such that, $\forall y \in \mathbb{R}_+^*$,

$$f(y) = \frac{A}{y} \tag{35}$$

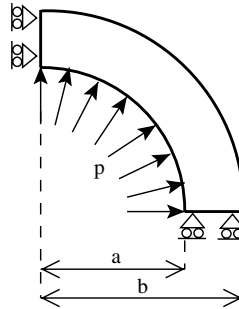


Fig. 9. Sphere under internal pressure.

and

$$A = A_1 - \nu A_2, \tag{36}$$

$$A_1 = af_y \left[\alpha^3 - \ln \alpha^2 - \frac{2}{3}(1 - \beta^3) \right]; \quad A_2 = af_y \left[\alpha^3 - \ln \alpha^4 - \frac{4}{3}(1 - \beta^3) \right], \tag{37}$$

$$\alpha = \frac{c}{a}; \quad \beta = \frac{c}{b}, \tag{38}$$

the constant c being obtained by solving the equation:

$$p = 2f_y \left[\ln \alpha + \frac{1}{3}(1 - \beta^3) \right]. \tag{39}$$

Table 2 provides the errors (expressed as a percentage (%)) on four statistical moments (mean, variance, skewness and kurtosis) for increasing qualities of the spline interpolation used for the computation of the approximation coefficients (see Eq. (16)).

For all the four moments, convergence of these errors on zero is observed when the number N_I of interpolation points increases. A very good accuracy of the mean is quickly obtained and not surprisingly, major efforts have to be made when the order of the statistical moments increases. Nevertheless, good results are obtained for all these four moments with a significant reduction of the number N_I of mechanical computations (here $N_I \leq 11$) by comparison with the 10^5 Monte Carlo simulations required.

Table 3 shows errors on variance, skewness and kurtosis of Z , for different coefficients of variation of the “input” r.v. Y and for several values of the number of interpolation points ($N_I = 7, 9, 11$).

Even if, as expected, errors increase with the coefficient of variation (the higher the moment order, the higher this phenomenon), less than 1% error has been obtained using appropriate spline interpolation (here $N_I = 11$, i.e. a 10-arcs spline was used on the interpolation domain).

Then, the Probability Density Function (PDF) of the response Z has been considered. This PDF has been obtained using two different ways. On the one hand, the PDF (called “analytical” in Fig. 10) has been estimated performing 10000000 simulations of the exact solution of the mechanical problem. On the other hand, the PDF had been approximated performing the same number of Monte Carlo simulations of the approximated response \tilde{Z} (18). We can observe in Fig. 10 that a good accuracy is obtained for an interpolation points number greater or equal to 9 (on the graph, the 11-points curve is superposed on the analytical one). Thus, using the proposed approximation technique, only 9 or 11 deterministic FE computations of the mechanical response are required for this problem (one for each interpolation point), whereas several millions of computations are needed using classical Monte Carlo simulations.

Table 2
Errors (%) on statistical moments ($\nu_Y = 0.3$)

	N_I							
	4	5	6	7	8	9	10	11
Mean	10.43	2.11	0.48	0.24	0.04	<0.01	<0.01	<0.01
Variance	19.17	27.15	8.59	0.91	1.38	0.34	0.06	0.03
Skewness	143.39	66.99	21.69	14.77	2.25	0.86	0.34	0.47
Kurtosis	140.07	192.76	268.15	29.14	12.15	10.00	2.21	0.62

Table 3
Errors (%) on statistical moments for various coefficients of variation

		Coefficients of variation					
		0.05	0.1	0.2	0.3	0.4	0.5
Variance	$N_I = 7$	0.81	0.83	0.88	0.91	0.86	0.70
	$N_I = 9$	0.10	0.12	0.20	0.34	0.57	0.90
	$N_I = 11$	<0.01	<0.01	0.01	0.03	0.06	0.10
Skewness	$N_I = 7$	10.67	10.76	12.27	14.77	17.78	20.65
	$N_I = 9$	0.64	0.98	1.04	0.86	0.40	0.44
	$N_I = 11$	0.78	0.44	0.38	0.47	0.62	0.78
Kurtosis	$N_I = 7$	2.53	3.62	9.58	29.14	93.17	288.60
	$N_I = 9$	0.38	0.51	1.99	10.00	42.28	145.92
	$N_I = 11$	0.14	0.20	0.39	0.62	0.72	0.38

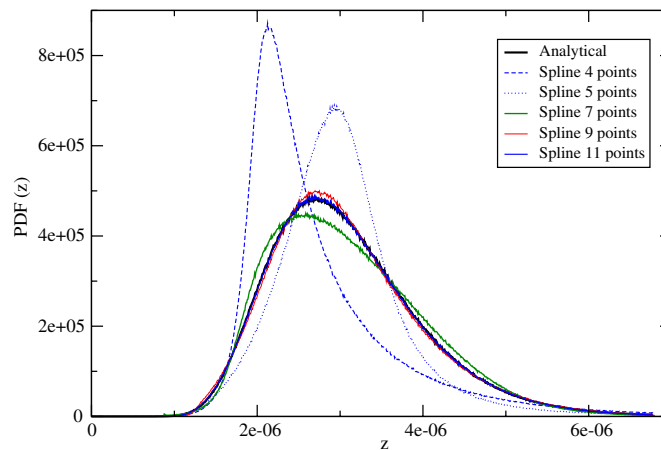


Fig. 10. Sphere—probability density functions.

3.4. Hertz contact problem

We eventually consider a Hertz contact problem between an infinitely long cylinder and a fixed rigid horizontal plane. The cylinder is compressed by a vertical uniform load $2F$ along its axis. The behavior of its material is supposed to be isotropic linear elastic in a first model (Section 3.4.1) and then elasto-plastic in a second one (Section 3.4.2). Plane strain assumption is made, so the analysis can be reduced to a two-dimensional one (see Fig. 11a).

Thanks to the problem symmetry, only half section of the cylinder, submitted to a load F , is discretized, using linear plain strain Finite Elements (see Fig. 11b). Contact is taken into account using a mesh of contact FE linking the basis of the cylinder and the portion of the plane that may be in contact. Due to the contact, the mechanical problem is nonlinear in both models (elastic and elasto-plastic ones) and the FE resolution is incremental and iterative.

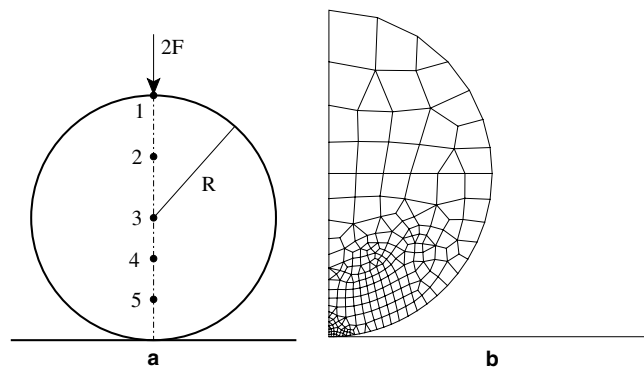


Fig. 11. Hertz contact problem—(a) geometry, (b) FE mesh.

We are interested in vertical displacements (z_i) of five points i ($1 \leq i \leq 5$) of the section S ($\mathbf{1}=(0, 2R)$, $\mathbf{2}=(0, \frac{3}{2}R)$, $\mathbf{3}=(0, R)$, $\mathbf{4}=(0, \frac{2}{3}R)$, $\mathbf{5}=(0, \frac{1}{3}R)$, see Fig. 11a). These displacements are gathered in a vector \mathbf{z} . They are set at five successive loading steps: $(F_i = 0, 2i \times F)_{1 \leq i \leq 5}$.

Parameters of the deterministic model, namely the Poisson’s ratio ν , the half-loading intensity F , the radius R and the yield limit stress f_y (for second model only), are equal to: $\nu = 0.3$; $F = 5000$ N; $R = 50$ mm; $f_y = 30 \times 10^6$ Pa.

3.4.1. Elastic cylinder

The uncertain parameter of this first model is the Young Modulus E of the constituent material, modeled by a lognormal r.v. Y , whose mean and coefficient of variation write respectively: $m_Y = 3 \times 10^{10}$ Pa; $v_Y = 0.2$. As a result, the vector displacements \mathbf{z} is a vector r.v. that we shall denote by $\mathbf{Z} = (Z_1, \dots, Z_5)$.

Tables 4a and 4b provide errors (expressed as a percentage (%)) on statistical moments, for $v_Y = 0.2$, for several values of the number N_I of interpolation points and for each r.v. $(Z_i)_{1 \leq i \leq 5}$. Table 4a shows errors on mean and variance. This table illustrates the very fast convergence of the mean errors on zero: only five interpolation points are required to obtain less than 1% error, whatever the r.v. Z_i .

Convergence of the variance errors is less easy, but about 2% errors are obtained for more than six interpolation points. Table 4b provides errors on skewness and kurtosis. Whatever the r.v. Z_i , we notice a good convergence of errors on zero. For both statistical moments, at most 5% errors (and in most cases, about 2% errors) are obtained for more than 7 interpolation points.

The probability density functions of the responses Z_i are then studied. Fig. 12a and b show the estimated PDFs of the r.v. Z_1 for the last loading step ($F_5 = F$). These PDFs had been obtained by Monte Carlo simulations of the approximated response \tilde{Z} (18). Different spline interpolations had been considered for the computation of the approximation coefficients. A convergence behavior is clearly observed in Fig. 12 for increasing interpolation points numbers (on this graph, 8 points spline and 11 points spline curves are quasi-superposed).

In Fig. 12b, these “approximated” PDFs are compared with the PDF estimated by direct Monte Carlo simulation of the deterministic FE model. Because of the high computational cost of this simulation, only 10^4 simulations had been made and 100 points of this PDF (called “exact” PDF) had been considered. By comparison, the “approximated” PDFs curves

Table 4a
Errors (%) on statistical moments ($v_Y = 0.2$): Mean and Variance—elastic cylinder

		N_I				
		4	5	6	8	11
Mean	Z_1	3.49	0.90	0.21	0.06	0.06
	Z_2	3.21	0.90	0.26	0.06	0.06
	Z_3	3.06	0.90	0.28	0.06	0.05
	Z_4	2.93	0.91	0.30	0.06	0.05
	Z_5	2.62	0.91	0.35	0.06	0.05
Variance	Z_1	3.23	22.83	7.10	1.77	2.13
	Z_2	2.48	23.23	6.87	2.01	2.11
	Z_3	2.06	23.46	6.75	2.15	2.10
	Z_4	1.70	23.66	6.63	2.27	2.09
	Z_5	0.86	24.14	6.35	2.56	2.07

Table 4b
Errors (%) on statistical moments ($v_Y = 0.2$): Skewness and Kurtosis—elastic cylinder

		N_I							
		4	5	6	7	8	9	10	11
Skewness	Z_1	138.36	36.73	27.61	11.02	1.89	0.79	0.76	0.63
	Z_2	139.13	35.93	30.50	10.58	2.60	0.56	0.72	0.94
	Z_3	139.44	35.38	32.28	10.32	3.09	0.45	0.67	1.13
	Z_4	139.64	34.85	33.94	10.10	3.57	0.36	0.61	1.31
	Z_5	139.75	33.29	38.26	9.56	4.91	0.18	0.40	1.78
Kurtosis	Z_1	77.97	62.81	110.71	9.00	1.91	1.34	1.67	0.83
	Z_2	74.60	60.72	121.99	9.46	1.24	2.02	1.72	0.80
	Z_3	72.65	59.54	128.77	9.76	0.90	1.98	1.79	0.74
	Z_4	70.90	58.50	134.96	10.06	0.62	1.71	1.86	0.65
	Z_5	66.62	56.01	150.48	10.86	0.07	0.41	2.10	0.13

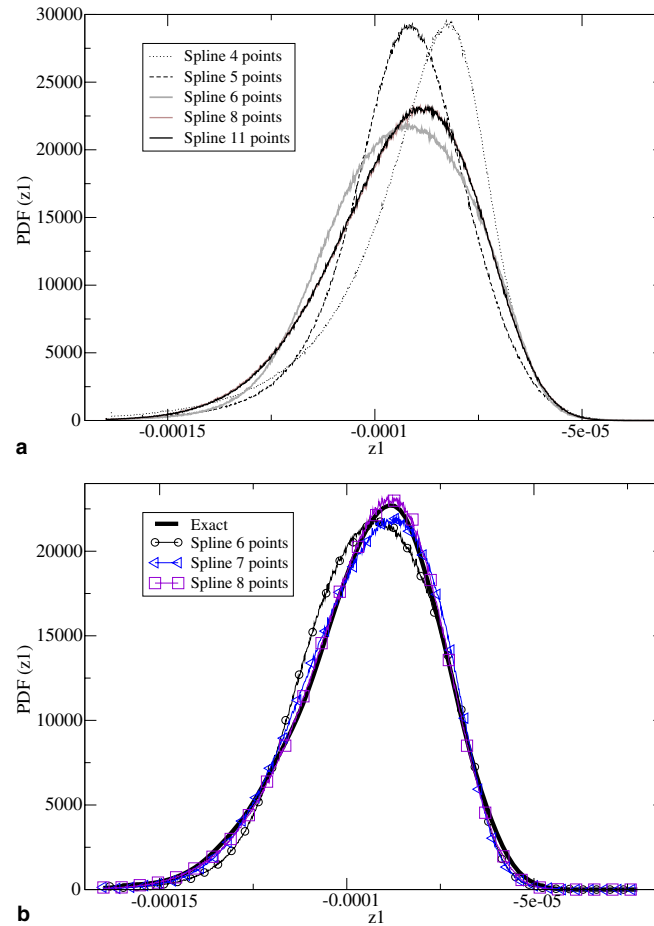


Fig. 12. Elastic cylinder—convergence of probability density functions displacement z_1 —loading step 5.

are 1000 points curves and had been obtained performing 10^7 simulations because 11 deterministic FE computations were at most needed in that case. In order to improve its shape, the “exact” PDF curve had been smoothed before being plotted in Fig. 12b. Despite the poor quality of the “exact” PDF, agreement of “exact” PDF and “approximated” ones for sufficient interpolation quality seems to be observed.

3.4.2. Elasto-plastic cylinder

Now we consider that the behavior of the cylinder is elasto-plastic with linear hardening. The uncertain parameters of this second model is the Young modulus E and the plastic modulus E_p , denoted afterwards y_1 and y_2 respectively. The couple (y_1, y_2) is modeled as a two-dimensional lognormal r.v. $Y = (Y_1, Y_2)$, with characteristics:

Mean of Y_1 and Y_2 : $m_{Y_1} = 3 \times 10^{10}$ Pa and $m_{Y_2} = 9 \times 10^9$ Pa.

Coefficient of variation of Y_1 and Y_2 : $v_{Y_1} = v_{Y_2} = 0.2$.

Coefficient of correlation of the couple: $\rho_{Y_1 Y_2} = 0.9$.

As a result, the vector displacements \mathbf{z} is a vector r.v. that we shall denote by $\mathbf{Z} = (Z_1, \dots, Z_5)$. The plastic points of the cylinder given by the deterministic FE computation with $E = y_1 = m_{Y_1}$ and $E_p = y_2 = m_{Y_2}$ are shown in Fig. 13 for the 5 loading steps considered. Tables 5a–5d provide errors (expressed as a percentage (%)) on statistical moments, for $v_{Y_1} = v_{Y_2} = 0.2$ and for several values of the number N_I of interpolation points ($(4 \times 4) \leq N_I \leq (11 \times 11)$), at two loading steps $F_1 = 0.2 \times F$ and $F_5 = F$, for each r.v. $(Z_i)_{1 \leq i \leq 5}$.

Table 5a illustrates the very fast convergence of the mean errors on zero: errors less than 1% error can easily be obtained whatever the r.v. Z_i and the load intensity.

Tables 5b–5d show the errors for moments of higher degrees (variance, skewness and kurtosis). As expected, accurate approximations of such moments require a higher computational effort. Nevertheless, satisfactory errors of 1–3% are obtained here for spline interpolations up to 8×8 points, whatever the r.v. Z_i and the loading level.

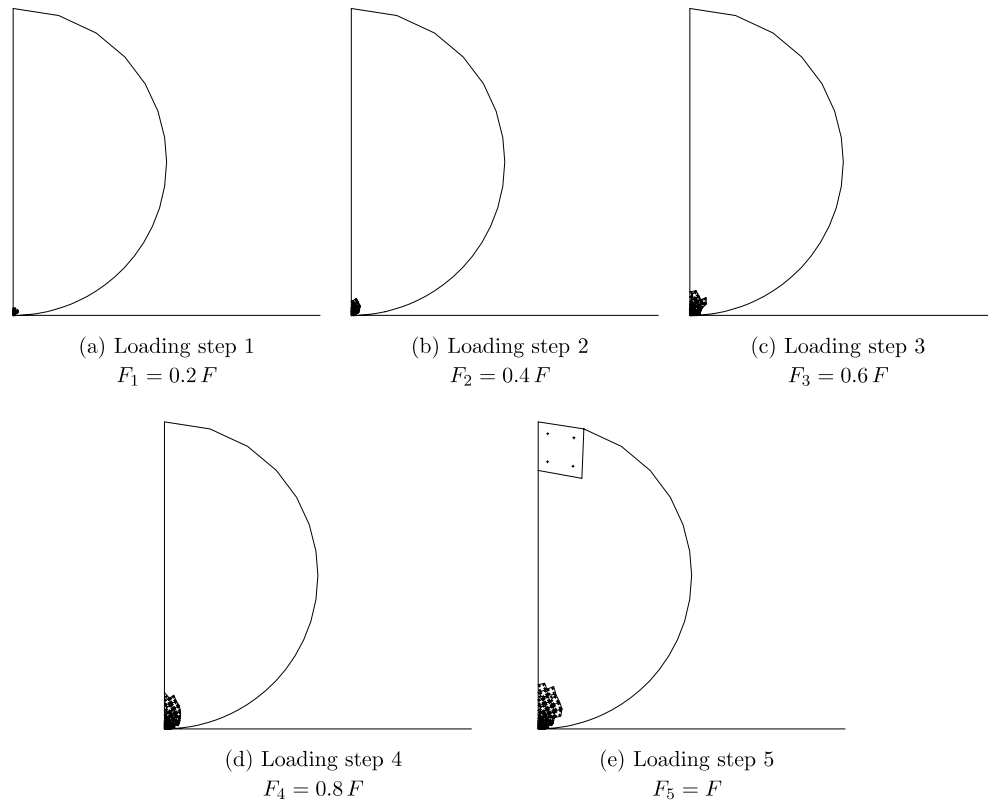


Fig. 13. Plastic points at different loading steps ($E = y_1 = m_{y_1}$, $E_p = y_2 = m_{y_2}$).

Table 5a
Errors (%) on Mean ($v_{y_1} = v_{y_2} = 0.2$)—elasto-plastic cylinder

			N_I				
			4×4	5×5	6×6	8×8	11×11
Mean	Z_1	Step 1	1.31	0.25	0.16	0.17	0.18
		Step 5	0.46	0.27	0.04	0.09	0.09
	Z_2	Step 1	1.19	0.21	0.19	0.20	0.20
		Step 5	0.08	0.24	0.03	0.09	0.09
	Z_3	Step 1	1.14	0.20	0.21	0.21	0.21
		Step 5	0.10	0.23	0.02	0.08	0.09
	Z_4	Step 1	1.09	0.18	0.23	0.22	0.23
		Step 5	0.25	0.22	0.02	0.08	0.09
	Z_5	Step 1	0.98	0.15	0.27	0.25	0.25
		Step 5	0.56	0.21	0.02	0.09	0.09

In Fig. 14 are plotted the “exact” and some “approximated” PDF of the r.v. Z_1 , for different accuracy of the interpolation ($N_I = 6 \times 6, 8 \times 8$), at the last loading step ($F_5 = F$). On the one hand, as simulations of approximated response \tilde{Z}_1 are very few time-consuming, 10^7 simulations were made for the “approximated” PDFs and these PDFs are plotted at 1000 points. On the other hand, because of the numerical cost of deterministic FE computations, the “exact” PDF results from 2×10^4 simulations only; Consequently, the corresponding curve is still a rather coarse approximation of the true one, as it can be seen for example by comparison between the estimated PDF and the associated smoothed curve. Nevertheless, despite the low resolution of the smoothed “exact” PDF, the “approximated” PDFs seem to be in satisfactory agreement with the “exact” one. The proposed approach is far less time-consuming, so 10^7 simulations of the PDF were made and these PDFs are plotted at 1000 points.

3.4.3. Comparison of the elastic and the elasto-plastic Hertz contact problems

In Fig. 15 are plotted three PDFs that correspond to the marginal law of r.v. Z_5 at the last loading step ($F_5 = F$). These PDFs have been evaluated by Monte Carlo simulations (10^7 simulations) of an accurate approximation involving a 11×11 interpolation points spline. The solid line curve shows the PDF for the elastic problem (Section 3.4.1: 1 r.v., the Young

Table 5b
Errors (%) on Variance ($v_{Y_1} = v_{Y_2} = 0.2$)—elasto-plastic cylinder

			N_I				
			4 × 4	5 × 5	6 × 6	8 × 8	11 × 11
Variance	Z_1	Step 1	1.17	6.64	3.63	2.47	2.67
		Step 5	0.86	6.47	5.24	2.76	3.10
	Z_2	Step 1	1.17	6.81	3.52	2.25	2.50
		Step 5	0.62	6.57	5.72	2.67	3.10
	Z_3	Step 1	1.16	6.90	3.46	2.13	2.40
		Step 5	0.47	6.63	5.97	2.64	3.11
	Z_4	Step 1	1.16	6.98	3.40	2.01	2.31
		Step 5	0.33	6.69	6.18	2.61	3.12
	Z_5	Step 1	1.15	7.18	3.25	1.72	2.08
		Step 5	0.03	6.85	6.62	2.55	3.13

Table 5c
Errors (%) on Skewness ($v_{Y_1} = v_{Y_2} = 0.2$)—elasto-plastic cylinder

			N_I				
			4 × 4	5 × 5	6 × 6	8 × 8	11 × 11
Skewness	Z_1	Step 1	40.12	2.60	5.33	1.92	1.65
		Step 5	19.40	2.21	15.07	2.28	2.59
	Z_2	Step 1	39.61	2.96	4.62	2.12	1.73
		Step 5	10.23	4.23	18.59	2.74	3.09
	Z_3	Step 1	39.33	3.17	4.21	2.24	1.78
		Step 5	5.30	5.43	20.55	3.03	3.37
	Z_4	Step 1	39.07	3.35	3.86	2.35	1.83
		Step 5	1.11	6.52	22.26	3.31	3.63
	Z_5	Step 1	38.44	3.78	2.99	2.63	1.96
		Step 5	8.06	9.17	26.15	4.02	4.23

Table 5d
Errors (%) on Kurtosis ($v_{Y_1} = v_{Y_2} = 0.2$)—elasto-plastic cylinder

			N_I				
			4 × 4	5 × 5	6 × 6	8 × 8	11 × 11
Kurtosis	Z_1	Step 1	20.58	10.23	2.48	2.07	2.66
		Step 5	11.49	7.49	0.49	1.46	2.33
	Z_2	Step 1	20.65	10.48	2.48	1.89	2.56
		Step 5	8.37	6.52	0.39	0.65	2.07
	Z_3	Step 1	20.69	10.62	2.47	1.78	2.51
		Step 5	6.84	5.98	0.88	0.05	1.91
	Z_4	Step 1	20.72	10.75	2.47	1.69	2.46
		Step 5	5.62	5.51	1.30	0.58	1.76
	Z_5	Step 1	20.80	11.04	2.46	1.43	2.31
		Step 5	3.19	4.45	2.22	2.45	1.42

modulus) and the dark curve with squares represents the PDF corresponding to the elasto-plastic problem (Section 3.4.2: 2 r.v., the Young modulus and the plastic modulus). An intermediate problem has also been considered: the cylinder is yet elasto-plastic but the randomness of the problem is only due to the Young modulus. The plastic modulus is then considered as equal to $m_{Y_2} = 9 \times 10^9$ Pa; the bright curve with circles represents the corresponding PDF.

Fig. 15 shows that, as it was expected, plastic behavior increases the (absolute value of the) vertical displacement. In the intermediate problem, we can observe that the response variance decreases by comparison to the elastic problem. On the contrary, if an additional source of randomness is included (namely the plastic modulus), the variance reaches a higher value.

Similar shapes of PDFs for these three problems can be seen if we consider the other r.v. of the response vector Z . These tendencies can also be observed and quantified in Tables 6a–6c. In Tables 6a–6c, columns (i), (ii) and (iv) give values corresponding respectively to the elastic, the intermediate and the elasto-plastic problems. In columns (iii) and (v), we can read relative growth or reduction rates (expressed as a percentage (%)) with respect to the elasticity problem.

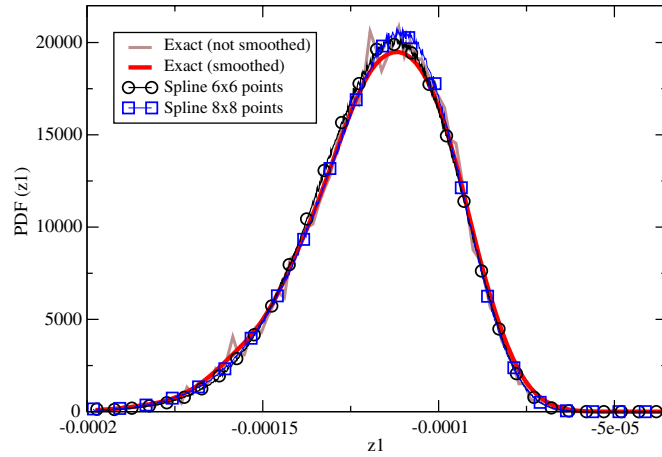


Fig. 14. Elasto-plastic cylinder—convergence of probability density functions displacement z_1 —loading step 5.

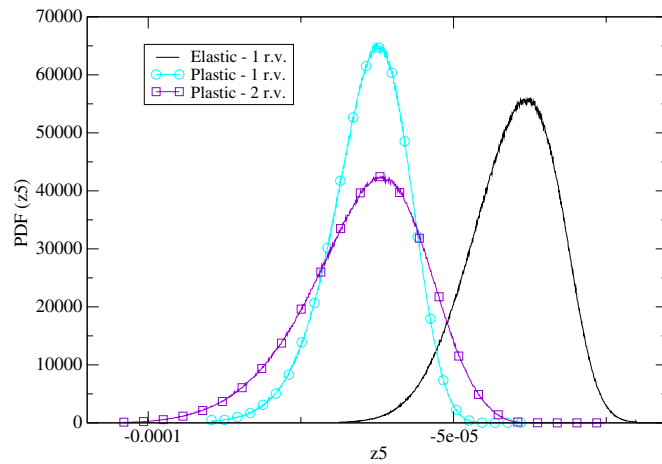


Fig. 15. Probability density functions 11×11 interpolation points—loading step 5.

Table 6a

Comparison of the (absolute value of the) means 11×11 interpolation points—loading step 5

r.v.	Elastic	Plastic 1 r.v.		Plastic 2 r.v.	
	(i)	(ii)	(iii)	(iv)	(v)
Z_1	9.37×10^{-5}	11.63×10^{-5}	+24%	11.70×10^{-5}	+25%
Z_2	6.59×10^{-5}	8.82×10^{-5}	+34%	8.89×10^{-5}	+35%
Z_3	5.66×10^{-5}	7.92×10^{-5}	+40%	7.99×10^{-5}	+41%
Z_4	5.05×10^{-5}	7.34×10^{-5}	+45%	7.41×10^{-5}	+47%
Z_5	4.02×10^{-5}	6.40×10^{-5}	+59%	6.47×10^{-5}	+61%

Table 6b

Comparison of the variances 11×11 interpolation points—loading step 5

r.v.	Elastic	Plastic 1 r.v.		Plastic 2 r.v.	
	(i)	(ii)	(iii)	(iv)	(v)
Z_1	31.76×10^{-11}	29.37×10^{-11}	-8%	41.09×10^{-11}	+29%
Z_2	15.06×10^{-11}	13.26×10^{-11}	-12%	21.51×10^{-11}	+43%
Z_3	10.85×10^{-11}	9.34×10^{-11}	-14%	16.55×10^{-11}	+53%
Z_4	8.43×10^{-11}	7.13×10^{-11}	-15%	13.70×10^{-11}	+62%
Z_5	5.09×10^{-11}	4.13×10^{-11}	-19%	9.67×10^{-11}	+90%

Table 6c

Comparison of the (absolute value of the) coefficients of variation 11×11 interpolation points—loading step 5

r.v.	Elastic	Plastic 1 r.v.		Plastic 2 r.v.	
	(i)	(ii)	(iii)	(iv)	(v)
Z_1	0.1904	0.1473	–23%	0.1732	–9%
Z_2	0.1861	0.1306	–30%	0.1650	–11%
Z_3	0.1839	0.1221	–34%	0.1611	–12%
Z_4	0.1820	0.1151	–37%	0.1580	–13%
Z_5	0.1774	0.1005	–43%	0.1520	–14%

The increase of the (absolute value of the) means when plasticity is taken into account, is found again in Table 6a for each r.v. $(Z_i)_{(i=1, \dots, 5)}$. We can see in Table 6b, that variances decrease for intermediate problem and not surprisingly increase for 2 r. v. elasto-plastic problem.

We can also observe that the amplitudes of the variations of these statistical moments increase from point 1 to point 5 (that is, when points are closer to the contact area). But no evident links appear between the plastic zone locations (at last loading step, point 1 stays in a plastic zone and point 5 is close to the other plastic zone (see Fig. 13)) and the variations of the statistical moments.

Finally, Table 6c deals with the coefficients of variation of the response r.v. In the elastic case, these coefficients of variation are close to the coefficient of variation of the input r.v. ($v_Y = 0.2$). On the contrary, elasto-plasticity produces a decrease of the coefficients of variation; this decreasing tendency is observed even if an additional source of randomness is taken into account (plasticity with 2 r.v.).

4. Conclusion

This paper is a contribution to the development of SFE Methods for nonlinear mechanical problems. The presented approach is the combination of two techniques: (i) the expansion of the mechanical nonlinear response on an Hilbertian basis, (ii) the calculations of the expansion coefficients thanks to a cubic B-spline interpolation. The application of this interpolation technique is original in the context of SFE Methods and leads to preliminary interesting results: accurate approximations of the response on the whole definition domain are obtained from a limited number of calls of the finite element model. The coefficients of this expansion up to the expected order are then computed at low cost from the interpolation. The statistical moments of any order and the Probability Density Function (PDF) of the mechanical response can then be estimated in an economic way.

The proposed technique was tested on four examples. The first considered problem was mechanically linear and the three others were nonlinear (elasto-plastic material and contact problem in the fourth example). One or several (correlated) lognormal r.v. were considered on the different problems. The accuracy of the approximations was evaluated by comparison to reference solutions obtained whether by analytical models or by Monte Carlo simulations. The effect of the interpolation refinement and of the dimension space projection on the calculated moments were eventually studied.

Beyond the use of a mathematically convergent development, comparisons to target results show a satisfactory convergence of the Hilbertian expansion as soon as the spline interpolation is accurate enough. Concerning the presented applications, the method leads to exploitable and satisfactory results. However, these first results have to be confirmed on much more complex problems.

The proposed approach can be put among the family of the response surface methods: the canonic basis of polynomials used in classical regression techniques is here replaced by an orthogonal basis (namely the Hermite polynomials basis) and the Euclidean norm on \mathbb{R}^k is replaced by the norm associated to the space of v_k -square integrable functions from \mathbb{R}^k to \mathbb{R} defined in (9).

The response surface methods are widely developed, especially because they can be very easily coupled with existing deterministic FE codes. It has been already pointed out in the literature that they can be applied to a large class of engineering problems in a reliability context or for statistical moments computations in a sensitivity analysis context. Nevertheless, although these approaches are economical when compared to Monte Carlo simulations, it is clear that the computational cost will increase with the number of input r.v. Consequently, with current computational resources, it seems difficult to apply such methods, including the proposed approach, to problems involving random fields.

An important issue for response surface obtained by regression techniques is the storage and the inversion of the (usually ill-conditioned) matrix of the system that defines the approximation coefficients. However, thanks to the orthogonality of the Hermite polynomials, the corresponding matrix is here diagonal so these two difficulties disappear.

The second important problem is the evaluation of the integrals involved in the definition of the response surface coefficients. In this paper, an accurate cubic B-spline interpolation technique has been chosen. Alternatives, like efficient Monte

Carlo techniques or quadratures methods, can also be found in the literature (see [25,20]). Here, a unique approximation of the response surface is made. This is an important advantage of the proposed method because, unlike the above mentioned methods, as soon as an accurate enough B-spline interpolation is obtained, no additional mechanical computations would be needed for the approximation of moments of any order. Eventually, the location of the integration points has to be optimized. Here we considered, for simplicity, uniformly distributed points. It could be useful to test other strategies too (collocation technique, etc.).

We believe it would now be interesting to carry out comparisons, by help of some benchmarks, between these different ways, especially for high order moments computations.

Appendix A. Gaussian standardization of lognormal random vectors

Let $Y = (Y_1, \dots, Y_k)$ be a k -dimensional lognormal random variable with given mean $m_Y \in \mathbb{R}^k$ and covariance matrix $C_Y \in \mathbb{R}^{k \times k}$, such that

$$m_Y = \begin{bmatrix} m_{Y_1} \\ m_{Y_2} \\ \vdots \\ m_{Y_k} \end{bmatrix}; \quad C_Y = \begin{bmatrix} \sigma_{Y_1}^2 & C_{Y_1Y_2} & \cdots & C_{Y_1Y_k} \\ C_{Y_2Y_1} & \sigma_{Y_2}^2 & \cdots & C_{Y_2Y_k} \\ \vdots & \vdots & \ddots & \vdots \\ C_{Y_kY_1} & C_{Y_kY_2} & \cdots & \sigma_{Y_k}^2 \end{bmatrix}, \tag{A.1}$$

where, $\forall (i,j) \in \{1, \dots, k\}^2$,

$$m_{Y_i} = \langle Y_i \rangle; \quad \sigma_{Y_i}^2 = C_{Y_iY_i}; \quad C_{Y_iY_j} = \langle (Y_i - m_{Y_i})(Y_j - m_{Y_j}) \rangle. \tag{A.2}$$

Let $\Gamma \in \mathbb{R}^{k \times k}$ be the symmetric and positive-definite ($k \times k$) real matrix whose generic term Γ_{ij} is given by

$$\Gamma_{ij} = \ln \left(1 + \frac{C_{Y_iY_j}}{m_{Y_i}m_{Y_j}} \right), \quad (i,j) \in \{1, \dots, k\}^2. \tag{A.3}$$

Let $L \in \mathbb{R}^{k \times k}$ be the lower triangular ($k \times k$) real matrix derived from Cholesky’s factorization of Γ :

$$\Gamma = LL^T. \tag{A.4}$$

Let $T: x = (x_1, \dots, x_k) \rightarrow y = (y_1, \dots, y_k) = T(x)$ be the function from \mathbb{R}^k into \mathbb{R}^k defined by

$$y = T(x) \iff \begin{cases} y_1 = \frac{m_{Y_1}}{\sqrt{1 + v_{Y_1}^2}} \exp\{(Lx)_1\} \\ \vdots \\ y_k = \frac{m_{Y_k}}{\sqrt{1 + v_{Y_k}^2}} \exp\{(Lx)_k\} \end{cases} \tag{A.5}$$

where $v_{Y_i} = \sigma_{Y_i}m_{Y_i}^{-1}$ is the coefficient of variation of Y_i and $(Lx)_i$ is the i th component of the vector Lx on the canonic basis of \mathbb{R}^k .

Finally, let $X = (X_1, \dots, X_k)$ be a k -dimensional standard Gaussian random variable, i.e. a \mathbb{R}^k -valued Gaussian random variable with zero mean and unit covariance matrix.

Then, we have the following result: the random variables Y and $T(X)$ have the same probability distribution, i.e.:

$$Y \stackrel{\mathcal{L}}{=} T(X), \tag{A.6}$$

where the symbol $\stackrel{\mathcal{L}}{=}$ denotes the equality of probability distributions.

As an example, the above relation takes the following forms for $k = 1$ and $k = 2$:

- *Scalar case ($k = 1$):*

$$Y = T(X) = \frac{m_Y}{\sqrt{1 + v_Y^2}} \exp\{LX\} \tag{A.7}$$

with

$$L = \sqrt{\ln(1 + v_Y^2)}. \tag{A.8}$$

• *Two-dimensional case* ($k = 2$):

$$Y = T(X) \iff \begin{cases} Y_1 = \frac{m_{Y_1}}{\sqrt{1 + v_{Y_1}^2}} \exp\{L_{11}X_1\} \\ Y_2 = \frac{m_{Y_2}}{\sqrt{1 + v_{Y_2}^2}} \exp\{L_{21}X_1 + L_{22}X_2\} \end{cases} \tag{A.9}$$

with:

$$L_{11} = \sqrt{\ln(1 + v_{Y_1}^2)} \tag{A.10}$$

$$L_{21} = \frac{\ln(1 + \rho_{Y_1Y_2} v_{Y_1} v_{Y_2})}{\sqrt{\ln(1 + v_{Y_1}^2)}} \tag{A.11}$$

$$L_{22} = \sqrt{\frac{\ln(1 + v_{Y_1}^2) \ln(1 + v_{Y_2}^2) - \ln^2(1 + \rho_{Y_1Y_2} v_{Y_1} v_{Y_2})}{\ln(1 + v_{Y_1}^2)}} \tag{A.12}$$

where $\rho_{Y_1Y_2} = C_{Y_1Y_2}(\sigma_{Y_1}\sigma_{Y_2})^{-1}$ is the coefficient of correlation of the couple (Y_1, Y_2) .

Appendix B. Hermite polynomials on \mathbb{R}^k

Let us recall first that the family $(H_m, m \in \mathbb{N})$ of the Hermite polynomials on \mathbb{R} (i.e. $x \in \mathbb{R}$) is defined by

$$H_m(x) = \begin{cases} 1 & \text{if } m = 0, \\ (-1)^m e^{\frac{x^2}{2}} \frac{d^m}{dx^m} (e^{-\frac{x^2}{2}}) & \text{if } m \in \mathbb{N}^*, \end{cases} \tag{B.1}$$

and satisfies the recurrence relationship:

$$H_0(x) = 1; \quad H_{m+1}(x) = xH_m(x) - H'_m(x). \tag{B.2}$$

As an example, the six first Hermite polynomials on \mathbb{R} are

$$\begin{aligned} H_0(x) &= 1, & H_3(x) &= x^3 - 3x, \\ H_1(x) &= x, & H_4(x) &= x^4 - 6x^2 + 3, \\ H_2(x) &= x^2 - 1, & H_5(x) &= x^5 - 10x^3 + 15x. \end{aligned}$$

These polynomials are orthogonal with respect to the standard Gaussian measure ν on \mathbb{R} :

$$\forall (m, n) \in \mathbb{N}^2, \quad \int_{-\infty}^{+\infty} H_n(x)H_m(x)\nu(dx) = n!\delta_{nm}. \tag{B.3}$$

Let $h_m(x)$ be the polynomial on \mathbb{R} —called the m -order standardized Hermite polynomial on \mathbb{R} —such that, $\forall m \in \mathbb{N}$:

$$h_m(x) = \frac{1}{\sqrt{m!}} H_m(x). \tag{B.4}$$

The family $(h_m(x), m \in \mathbb{N})$ satisfies

$$\forall (m, n) \in \mathbb{N}^2, \quad \int_{-\infty}^{+\infty} h_n(x)h_m(x)\nu(dx) = \delta_{nm} \tag{B.5}$$

and forms an orthonormal basis of the Hilbert space $L^2(\mathbb{R}, \nu)$ [24].

Let $\alpha = (\alpha_1, \dots, \alpha_k) \in \mathbb{N}^k$, $k \in \mathbb{N}^*$, be a k -order multi-index with length $|\alpha| = \alpha_1 + \dots + \alpha_k$, and let $\alpha!$ and $\delta_{\alpha,\beta}$ be the symbols defined by

$$\alpha! = \alpha_1! \times \dots \times \alpha_k!; \quad \forall (\alpha, \beta) \in \mathbb{N}^k \times \mathbb{N}^k, \quad \delta_{\alpha,\beta} = \delta_{\alpha_1\beta_1} \times \dots \times \delta_{\alpha_k\beta_k}, \tag{B.6}$$

where $\alpha_j!$ and $\delta_{\alpha_j\beta_j}$ are the common factorial and Kronecker’s delta symbols.

Then, the α -order Hermite polynomial on \mathbb{R}^k (i.e. $x \in \mathbb{R}^k$) is defined by

$$H_\alpha(x) = \prod_{i=1}^k H_{\alpha_i}(x_i), \tag{B.7}$$

where $x = (x_1, \dots, x_k)$ and, $\forall i \in \{1, \dots, k\}$, $H_{\alpha_i}(x_i)$ is the α_i -order Hermite polynomial on \mathbb{R} . Hermite polynomials on \mathbb{R}^k are orthogonal with respect to the standard Gaussian measure v_k on \mathbb{R}^k :

$$\forall (\alpha, \beta) \in \mathbb{N}^k \times \mathbb{N}^k, \int_{\mathbb{R}^k} H_\alpha(x)H_\beta(x)v_k(dx) = \alpha!\delta_{\alpha,\beta}. \tag{B.8}$$

Let $h_\alpha(x)$ be the polynomial on \mathbb{R}^k —called the α -order standardized Hermite polynomial on \mathbb{R}^k —such that, $\forall \alpha \in \mathbb{N}^k$:

$$h_\alpha(x) = \frac{1}{\sqrt{\alpha!}}H_\alpha(x). \tag{B.9}$$

The family $(h_\alpha(x), \alpha \in \mathbb{N}^k)$ satisfies

$$\forall (\alpha, \beta) \in \mathbb{N}^k \times \mathbb{N}^k, \int_{\mathbb{R}^k} h_\alpha(x)h_\beta(x)v_k(dx) = \delta_{\alpha,\beta}, \tag{B.10}$$

and forms an orthonormal basis of the Hilbert space $L^2(\mathbb{R}^k, v_k)$.

Let us recall that the standard Gaussian measure v_k on \mathbb{R}^k is defined as

$$v_k(dx) = (2\pi)^{-\frac{k}{2}} \exp\left(-\frac{\|x\|^2}{2}\right) dx, \tag{B.11}$$

where $x = (x_1, \dots, x_k)$ and $dx = dx_1 \cdots dx_k$. For $k = 1$, v_1 is denoted by v .

Appendix C. Cubic B-spline interpolation

- *Functions from \mathbb{R} into \mathbb{R} .*

Let a and b be two real numbers such that $-\infty < a < b < +\infty$, and let f be a function from \mathbb{R} into \mathbb{R} such that $Def(f) \subseteq [a, b]$, where $Def(f)$ denotes the definition domain of f . We consider a partition $[x_0, x_1[\cup \dots \cup [x_{n-1}, x_n[\cup [x_n, x_{n+1}]$ of $[a, b]$, where $x_0 = a$ and $x_{n+1} = b$, and we suppose that the values $(f(x_i); i = 0, \dots, n + 1)$ of f at the $n + 2$ nodes x_i of this partition are known (thanks to a first calculation). We want then to approximate f on $[a, b]$ by a cubic B-spline function S satisfying the $n + 2$ interpolation conditions:

$$S(x_i) = f(x_i), \quad i \in \{0, \dots, n + 1\}. \tag{C.1}$$

According to the B-spline interpolation technique, the target approximation S is of the form [7]:

$$S(x) = \sum_{l=0}^{n+3} P_l N_3^l(x), \tag{C.2}$$

where the $n + 4$ real functions N_3^l are the cubic B-spline basis functions associated with the nodal vector $(t_0, t_1, \dots, t_{n+7})$, with $t_0 = t_1 = t_2 = t_3 = x_0$, $t_4 = x_1, \dots, t_{n+3} = x_n$, and $t_{n+4} = t_{n+5} = t_{n+6} = t_{n+7} = x_{n+1}$.

For this nodal vector, the $n + 6$ B-spline basis functions of degree 0 are given by

$$\begin{cases} N_0^0(x) = N_0^1(x) = N_0^2(x) \equiv 0, \\ N_0^l(x) = \mathbb{1}_{[t_l, t_{l+1}[}(x) = \mathbb{1}_{[x_{l-3}, x_{l-2}[}(x) \quad \text{for } l = 3, \dots, n + 3, \\ N_0^{n+4}(x) = N_0^{n+5}(x) = N_0^{n+6}(x) \equiv 0, \end{cases} \tag{C.3}$$

and, for $0 \leq l \leq n + 6 - k$, the basis functions N_k^l of degree k can be obtained using the following recurrence formula:

$$N_k^l(x) = \frac{x - t_l}{t_{l+k} - t_l} N_{k-1}^l(x) + \frac{t_{l+k+1} - x}{t_{l+k+1} - t_{l+1}} N_{k-1}^{l+1}(x). \tag{C.4}$$

Because the extreme nodes are of multiplicity 4 ($t_0 = t_1 = t_2 = t_3 = x_0$ and $t_{n+4} = t_{n+5} = t_{n+6} = t_{n+7} = x_{n+1}$), the following conditions must be satisfied:

$$P_0 = f(x_0); \quad P_{n+3} = f(x_{n+1}); \quad 3 \times \frac{P_1 - P_0}{x_1 - x_0} = \frac{df}{dx}(x_0); \quad 3 \times \frac{P_{n+3} - P_{n+2}}{x_{n+1} - x_n} = \frac{df}{dx}(x_n). \tag{C.5}$$

In practice, the derivative $\frac{df}{dx}(x_0)$ and $\frac{df}{dx}(x_n)$ are usually unknown but can be approximated using a numerical differentiation scheme.

Finally, the n unknown coefficients P_2, P_3, \dots, P_{n+1} are obtained by solving the following linear system:

$$\begin{cases} b_1 P_2 + c_1 P_3 & = (d_0 + d_1)f(x_1) - a_1 P_1 \\ a_2 P_2 + b_2 P_3 + c_2 P_4 & = (d_1 + d_2)f(x_2) \\ \vdots & \vdots \\ a_{n-1} P_{n-1} + b_{n-1} P_n + c_{n-1} P_{n+1} & = (d_{n-2} + d_{n-1})f(x_{n-1}) \\ a_n P_n + b_n P_{n+1} & = (d_{n-1} + d_n)f(x_n) - c_n P_{n+2} \end{cases} \tag{C.6}$$

where

$$\begin{aligned} a_i &= \frac{(d_i)^2}{D_{i-1}}; & b_i &= \frac{d_i(d_{i-2} + d_{i-1})}{D_{i-1}} + \frac{d_{i-1}(d_i + d_{i+1})}{D_i}; & c_i &= \frac{(d_{i-1})^2}{D_i} \\ d_i &= x_{i+1} - x_i; & D_i &= d_{i-1} + d_i + d_{i+1} & \text{and} & d_{-1} = d_{n+1} = 0. \end{aligned} \tag{C.7}$$

• *Functions from \mathbb{R}^2 into \mathbb{R} .*

Let a, b, c and d be four real numbers such that $-\infty < a < b < +\infty$ and $-\infty < c < d < +\infty$, and let f be a function from \mathbb{R}^2 into \mathbb{R} such that $Def(f) \subseteq [a, b] \times [c, d]$. We consider a partition $[[x_0, x_1[\cup \dots \cup [x_{n-1}, x_n[\cup [x_n, x_{n+1}]]] \times [[y_0, y_1[\cup \dots \cup [y_{m-1}, y_m[\cup [y_m, y_{m+1}]]]]$ of $[a, b] \times [c, d]$, where $x_0 = a, x_{n+1} = b, y_0 = c$ and $y_{m+1} = d$, and we suppose that the values $(f(x_i, y_j); i = 0, \dots, n + 1; j = 0, \dots, m + 1)$ of f at the $(n + 2)(m + 2)$ nodes (x_i, y_j) of this partition are known. We want then to approximate f on $[a, b] \times [c, d]$ by a cubic B-spline function S satisfying the $(n + 2)(m + 2)$ interpolation conditions:

$$S(x_i, y_j) = f(x_i, y_j), \quad (i, j) \in \{0, \dots, n + 1\} \times \{0, \dots, m + 1\}. \tag{C.8}$$

The solution S is of the form:

$$S(x, y) = \sum_{l=0}^{n+3} \sum_{k=0}^{m+3} P_{lk} N_3^l(x) N_3^k(y), \tag{C.9}$$

where the real functions $(N_3^l)_{(0 \leq l \leq n+3)}$ and $(N_3^k)_{(0 \leq k \leq m+3)}$ are the cubic B-spline basis functions respectively associated with the nodal vectors $(x_0, x_0, x_0, x_0, x_1, \dots, x_n, x_{n+1}, x_{n+1}, x_{n+1}, x_{n+1})$ and $(y_0, y_0, y_0, y_0, y_1, \dots, y_m, y_{m+1}, y_{m+1}, y_{m+1}, y_{m+1})$. The above formula can also be written:

$$S(x, y) = \sum_{l=0}^{n+3} P_l(y) N_l(x) \tag{C.10}$$

with

$$P_l(y) = \sum_{k=0}^{m+3} P_{lk} N_k(y). \tag{C.11}$$

Thus, the two-dimensional interpolation problem leads to a set of $((m + 2) + (n + 4))$ one-dimensional interpolation problems.

It should be noticed that four additional boundary conditions are required in such a two-dimensional interpolation procedure. In practice, it leads to the evaluation of the four twists $\frac{\partial^2 f}{\partial x \partial y}(x_0, y_0), \frac{\partial^2 f}{\partial x \partial y}(x_{n+1}, y_0), \frac{\partial^2 f}{\partial x \partial y}(x_0, y_{m+1})$ and $\frac{\partial^2 f}{\partial x \partial y}(x_{n+1}, y_{m+1})$.

References

[1] M. Anders, M. Hori, Three dimensional stochastic finite element method for elasto-plastic bodies, *Int. J. Numer. Methods Engrg.* 51 (2001) 449–478.
 [2] S.K. Au, J.L. Beck, A new adaptative importance sampling scheme for reliability calculations, *Struct. Safety* 21 (1999) 135–158.
 [3] H. Baldeweck, Méthodes aux éléments finis stochastiques—Application à la géotechnique, Thèse de doctorat, Université d’Evry, 1999.
 [4] P. Bernard, M. Fogli, Une méthode de Monte Carlo performante pour le calcul de la probabilité de ruine, *Rev. CTICM* 4 (1987) 23–40.
 [5] C.G. Bucher, Adaptative sampling: an iterative fast Monte Carlo procedure, *Struct. Safety* 5 (1988) 119–126.
 [6] A.C. Cornell, First order uncertainty analysis of soils deformation and stability, *Proceedings, First conference on Applications of Statistics and Probability to Soil and Structural Engineering, Hong Kong* (1971) 130–144.
 [7] G. Demengel, J.P. Pouget, Modèles de Bézier, des B-splines et des Nurbs, *Ellipses*, 1998.
 [8] G. Deodatis, Weighted Integral Method I: stochastic stiffness matrix, *J. Engrg. Mech.* 117 (8) (1991) 1851–1864.
 [9] A. Der Kiureghian, H.Z. Lin, S.J. Hwang, Second order reliability approximations, *J. Engrg. Mech.* 113 (8) (1998) 1208–1225.

- [10] O. Ditlevsen, H.O. Madsen, *Structural Reliability Methods*, John Wiley, 1996.
- [11] L. Faravelli, Response-surface approach for reliability analysis, *J. Engrg. Mech.* 115 (1989) 2763–2781.
- [12] R.V. Field, M. Grigoriu, On the accuracy of the polynomial chaos approximation, *Prob. Engrg. Mech.* 19 (2004) 65–80.
- [13] R. Ghanem, Ingredients for a general purpose stochastic finite elements implementation, *Comput. Methods Appl. Mech. Engrg.* 168 (1999) 19–34.
- [14] R. Ghanem, P.D. Spanos, *Stochastic Finite Elements: A Spectral Approach*, Springer-Verlag, 1991.
- [15] Computational stochastic mechanics 4—Stochastic finite elements, *Probabilistic Mechanics* 12(4) (1997) 245–321.
- [16] S.S. Isukapalli, A. Roy, P.G. Georgopoulos, Stochastic Response Surface Methods (SRSMs) for uncertainty propagation: application to environmental and biological systems, *Risk Anal.* 18 (3) (1998) 351–362.
- [17] J. Lubliner, *Plasticity Theory*, Maxwell Macmillan International Editions, 1990.
- [18] J. Mandel, *Mécanique des milieux continus*, Gauthier-Villars, Paris, 1966.
- [19] H.G. Matthies, C.E. Brenner, C.G. Bucher, C. Guedes Soares, Uncertainties in probabilistic numerical analysis of structures and solids—stochastic finite elements, *Struct. Safety* 19 (3) (1997) 283–336.
- [20] H.G. Matthies, A. Keese, Galerkin methods for linear and nonlinear elliptic stochastic partial differential equations Special Issue on, *Comput. Methods Appl. Mech. Engrg.* 194 (2005) 1295–1331.
- [21] A. Mohamed, M. Lemaire, Improved response surface method by using second order sensitivity operators, *Proceedings of the ICASP8 1* (2000) 117–124.
- [22] M. Rosenblatt, Remarks on a multiformation, *Ann. Math. Statist.* 23 (1952) 470–472.
- [23] Y.A. Shreider, *The Monte Carlo Method*, Pergamon Press, 1966.
- [24] C. Soize, *Méthodes mathématiques en analyse du signal*, Masson, 1993.
- [25] S.A. Smolyak, Quadrature and interpolation formulas for tensors products of certain classes of functions, *Sov. Math. Dokl.* 4 (1963) 240–243.
- [26] G. Stefanou, M. Papadrakakis, Stochastic finite element analysis of shell with combined random material and geometric properties, *Comput. Methods Appl. Mech. Engrg.* 193 (2004) 139–160.
- [27] B. Sudret, A. Der Kiureghian, *Stochastic finite elements and Reliability. A State-of-the-Art Report*, Report No. UCB/SEMM-2000/08, Department of Civil Engineering University of California, Berkeley, 2000.